Stochastic Environmental Research and Risk Assessment (2021) 35:831–848
https://doi.org/10.1007/s00477-020-01948-0

ORIGINAL PAPER

Projections of precipitation over China based on CMIP6 models

Jiaxi Tian[1] · Zengxin Zhang[1,2] · Zeeshan Ahmed[2] · Leying Zhang[1] · Buda Su[3] · Hui Tao[2] · Tong Jiang[4]

Accepted: 25 November 2020 / Published online: 3 January 2021

Abstract

Precipitation fluctuations are continuously threatening the environment and may cause huge economic losses. In present study, the precipitation over China has been evaluated under five principal shared socioeconomic pathways (SSPs) scenarios during 2015–2099 based on eight CMIP6 models bias-corrected by the method of Equidistant Cumulative Distribution Functions. The results showed that (1) the simulated precipitation in China was in good agreement with observed precipitation for the eight CMIP6 models during 1961–2014, especially for the UKESM1-0-LL and MIROC6. However, the simulated annual mean precipitation has been significantly overvalued in the Southwest River basin (> 50%), while it was undervalued in the higher elevations of the Northwest River basin (< − 60%); (2) the annual mean precipitation will show a fluctuating upward trend during 2015–2099 over China under all the SSPs scenarios for the eight CMIP6 models. The rate of precipitation increase over north China will be higher than that in south China, especially in the Northwest River basin (reach 57.44% in the 2090s under the SSP5-8.5 for the ensemble mean). This increase of the precipitation in north China might alleviate the shortage of water there, but will not change the pattern of more rain in the south and less in the north; (3) in the southeastern basins, the precipitation of the multi-model ensemble (MME) and MIROC6 during 2011–2020 will be lower than that of 1961–2010 (− 6.53 to − 0.06%) under all SSPs scenarios. While the precipitation will increase obviously under all the SSPs scenarios, especially for the SSP5-8.5 scenario after the year of 2060; (4) the bias of the MME was much lower than that of individual CMIP6 models, and the bias of lower SSPs scenarios will be relatively lower. Generally, uncertainty ranges of precipitation fluctuations in north China (15.31–79.26%) will be higher than those in south China (16.06–7.55%). These findings revealed the projections and uncertainties of CMIP6 precipitation over China, which will be helpful for a better understanding of the future evolution of precipitation in China at large scale and in other regions of the world.

Keywords CMIP6 · Precipitation · SSPs · Large river basin · China

✉ Zengxin Zhang
nfuzhang@163.com

Jiaxi Tian
tianjiaxi@njfu.edu.cn

Zeeshan Ahmed
zeeshanagronomist@yahoo.com

Leying Zhang
zhangleyingzi@126.com

Buda Su
subd@cma.gov.cn

Hui Tao
taohui@ms.xjb.ac.cn

Tong Jiang
jiangtong@cma.gov.cn

[1] Joint Innovation Center for Modern Forestry Studies, College of Biology and the Environment, Nanjing Forestry University, Nanjing 210037, Jiangsu, China

[2] Xinjiang Institute of Ecology and Geography, Chinese Academy of Sciences, Urumqi 830011, Xinjiang, China

[3] National Climate Centre, China Meteorological Administration, Beijing 100081, China

[4] School of Geographical Sciences, Nanjing University of Information Sciences and Technology, Nanjing 210044, Jiangsu, China

1 Introduction

Climate change and associated precipitation fluctuations can drastically influence human society, their surrounding environment, and the ecosystem, mainly by triggering extreme hydrological events like floods and droughts thus damaging the natural environment resulting in huge economic losses (Chen and Frauenfeld 2014; Zhou and Jiang 2017; Han et al. 2018). Therefore, robust precipitation projection is highly important to ensure water resources required for human survival and to safeguard water security in the context of changing climate. Owing to a clear understanding about physical processes of climate system and recent development and progress in modeling, the use of general circulation model (GCM) has become a major and vital tool for precipitation change studies.

However, due to model structural errors and parameterization uncertainty, the results of climate model integrations revealed substantial bias in the spatial and temporal distribution of regional precipitation (Steinschneider and Lall 2015). Therefore, it is necessary to select a model that could effectively simulate regional climate in the past and future scenarios (Wu et al. 2017). Recently, many researchers have evaluated the precipitation variability in different areas of the world using the Coupled Model Intercomparison Project (CMIP) datasets. For instance, Chen and Frauenfeld (2014) reported that they built a standard experimental protocol to estimate the atmosphere-ocean GCMs and to evaluate future climate predictions under different scenarios using the CMIP executed by the World Climate Research Programme (WCRP). Wang and Chen (2013a) revealed that the systematic error in reproducing precipitation was 8.1–88.5 mm based on the calendar months and the outcomes from 35 CMIP5 models. Sun et al. (2015) found that most CMIP5 models tended to overestimate precipitation over China, and this overestimation might be more serious in CMIP5 than that in CMIP3 (Chen and Frauenfeld 2014). Recently, the advanced climate prediction data has been provided by the sixth phase of the CMIP (CMIP6), and it features an increase in institutions, enhancements in spatial resolution, improvements in physical parameterizations and inclusion of additional Earth system processes and components (Eyring et al. 2019). A primary difference between CMIP5 and CMIP6 is the set of future scenarios used to project climate evolution (Editorial 2019). The CMIP5 implemented four Representative Concentration Pathways (RCPs). These four RCPs were a set of new pathways developed for the climate modeling community, which defined for the radiative forcing values reached by 2100 (van Vuuren et al. 2011). In contrast, the CMIP6 employed a new scenario framework rooted in socioeconomic trajectories: the shared socioeconomic pathways (SSPs), in which RCPs have been combined with alternative pathways of socioeconomic development (Editorial 2019; O'Neill et al. 2013). Also, the CMIP6 shows advantages in the expansion and endorsement of Model Intercomparison Projects (MIPs) focused on the bias, processes, and feedbacks in climate models (Heinze et al. 2019). Hence, the future scenarios of CMIP6 seem to be more reasonable in the new archive, especially the multimodel ensemble (MME) result, necessitating more research to evaluate their precipitation predictions.

Since the output of one single global climate model is always biased and uncertain, it cannot predict the trend of future climate accurately (Wu et al. 2017). Numerous studies emphasized that the MME technique is an effective way to reduce the uncertainty of independent models thereby improving predictions and their credibility (Feng et al. 2011; He et al. 2018; Sun et al. 2015; Katiraie-Boroujerdy et al. 2019) described that simulated precipitation of MME was much superior compared to the single CMIP5 model. In another study, He et al. (2018) estimated future extreme heat stress on rice in southern China, and found that the trend of observations generated through MME projections was much better than any individual general circulation model. The performance of MME is superior to the average single-model performance mainly because of error cancellation and non-linearity of the diagnostics (Hagedorn et al. 2005). Thus, interannual variations are huge in independent models but suppressed in the MME (Knutti and Sedláček 2013). As the number of models used in the MME increases, the ensemble results will be more accurate (Feng et al. 2011). Moreover, a number of schemes were applied to optimize the MME approach. Wang et al. (2014) explored the future patterns of extreme climatic events under different emission scenarios through MME projections by using the Bayesian Model Average method in the Haihe River Basin. Based on the independent component analysis and regularized regression approach, Lim et al. (2014) proposed an improved MME method to predict future precipitation in boreal summer over global and regional scales.

China is a vast country with complex terrain, and the precipitation in China varies greatly over space and time. Numerous country-scale studies have focused on the precipitation trend over China in the past decades. Gemmer et al. (2004) analyzed the monthly precipitation trends of 160 stations in China during 1951–2002, and discovered a clustering of trends in certain months, including distinct trend belts especially in east and northeast China. Chen and Frauenfeld (2014) indicated that precipitation increased over parts of northwestern China and decreased over the Tibetan Plateau throughout the twentieth century based on observed data. An analysis of the spatiotemporal changes

of precipitation extremes at 200 representative weather stations of China during 1956–2015 revealed that daily rainfall intensity showed a significant increasing trend nationally (Zheng et al. 2019). However, Zhang et al. (2017) identified that the precipitation in the upper Sangkan basin did not show any trend from 1957 to 2012 by using the data from three weather stations located in Loess Plateau, China. Besides the observed data with different trends, the predicted precipitation trend of China in CMIP5 showed a consistently increasing trend, which is greater in northern China than in southern China (Chen and Frauenfeld 2014; Wang and Chen 2013a; Xu and Xu 2012). Based on MME of eight climate models in the Fourth Assessment Report (AR4) of the Intergovernmental Panel on Climate Change (IPCC), Wu and Yan (2013) predicted that the annual precipitation will increase during 2011–2040 over Huaihe River basin. Furthermore, Chen and Frauenfeld (2014) revealed that the RCP8.5 scenario showed the largest significant trend, while the RCP 2.6 scenario exhibited the smallest increases across all of China.

Although, numerous studies have analyzed the fluctuations in the past and future precipitation patterns in some regions of China, only a very few studies have been conducted to comprehensively visualize the spatiotemporal distribution of precipitation at a large scale based on bias-corrected CMIP6 models. Therefore, the goals of this study were: (1) to evaluate the performance of the simulated precipitation over China based on the latest GCM models; (2) to project the patterns of the temporal and spatial distribution of future precipitation over China under different SSPs scenarios using the bias-corrected CMIP6 data. The outcomes of this study could improve the precipitation forecasting in China that would be quite helpful for decision-makers to make precipitation-related disaster management plans, and the relevant methods and results also have certain reference significance for other countries or regions.

2 Data and methodology

2.1 Study area and data

China is located in eastern Asia and its climate is potentially dominated by monsoon winds with clear precipitation differences between winter and summer. Generally, most of the precipitation is concentrated in the summer. Differences in precipitation also appear concerning region mainly due to the extensive territory and complex topography in China. On the national level, precipitation decreases from southeast to northwest (Zhang et al. 2011).

China is the third-largest country in area in the world. The total length of China's rivers is around 420,000 km, and there are more than 1500 rivers with a drainage area of over 1000 km^2. There are nine large river basins in China, which are shown in Fig. 1. The uneven distribution of rivers in China is mainly attributed to the topography and climate. Most of the rivers are situated in the wet eastern monsoon climatic zone, directly flowing into the sea. Contrary to that, northwestern China is dry with little precipitation, where rivers are not connected to the sea (Zhang et al. 2011).

The observed data used in this study was the monthly gridded precipitation interpolated from 2472 meteorological stations of China for the period 1961–2014 with a spatial resolution of 0.5° × 0.5° (http://data.cma.cn/site/index.html). The modeled precipitation was from eight CMIP6 models with r1i1p1f1 run under five principal future emission scenarios (Table 1). The period 1961–2014 was designated as the historic period, and the period 2015–2099 was considered as the future period. The five future scenarios were SSP1-1.9, SSP1-2.6, SSP2-4.5, SSP3-7.0, and SSP5-8.5. The SSP1-1.9 scenario corresponded to a very low forcing level, with a probability of warming being below 1.5 °C in 2100 (Zhang et al. 2019). The emission profile of the SSP1-1.9 scenario is characterized by a rapid decline to zero and a long period of negative emissions for CO_2 (O'Neill et al. 2016). The SSP1-2.6 scenario represented the low ending range of future scenarios measured by its radiative forcing pathway. This scenario will produce a multi-model mean of significantly less than 2.0 °C warming by 2100, thus could support the 2 °C temperature rise target study (O'Neill et al. 2016; Zhang et al. 2019). The SSP2-4.5 scenario was considered as a medium stabilization scenario, while the SSP3-7.0 scenario corresponded to the medium to high end of the range of future forcing pathways. The SSP5-8.5 was a scenario that stabilizes radiative forcing at 8.5 Wm^{-2} in 2100, and considered to be a high radiative forcing scenario (O'Neill et al. 2016).

2.2 Methodology

Based on the bias between modeled and observed precipitation at each percentile, the Equidistant Cumulative Distribution Functions (EDCDF) was used for the bias correction of raw CMIP6 outputs. EDCDF assumes that the difference between observation and simulated precipitation in the training period maintains during the correction period for a given percentile (Su et al. 2018). The EDCDF approach could be written as:

$$\Delta = F_{oc}^{-1}(F_{ms}(x)) - F_{mc}^{-1}(F_{ms}(x)) \quad (1)$$

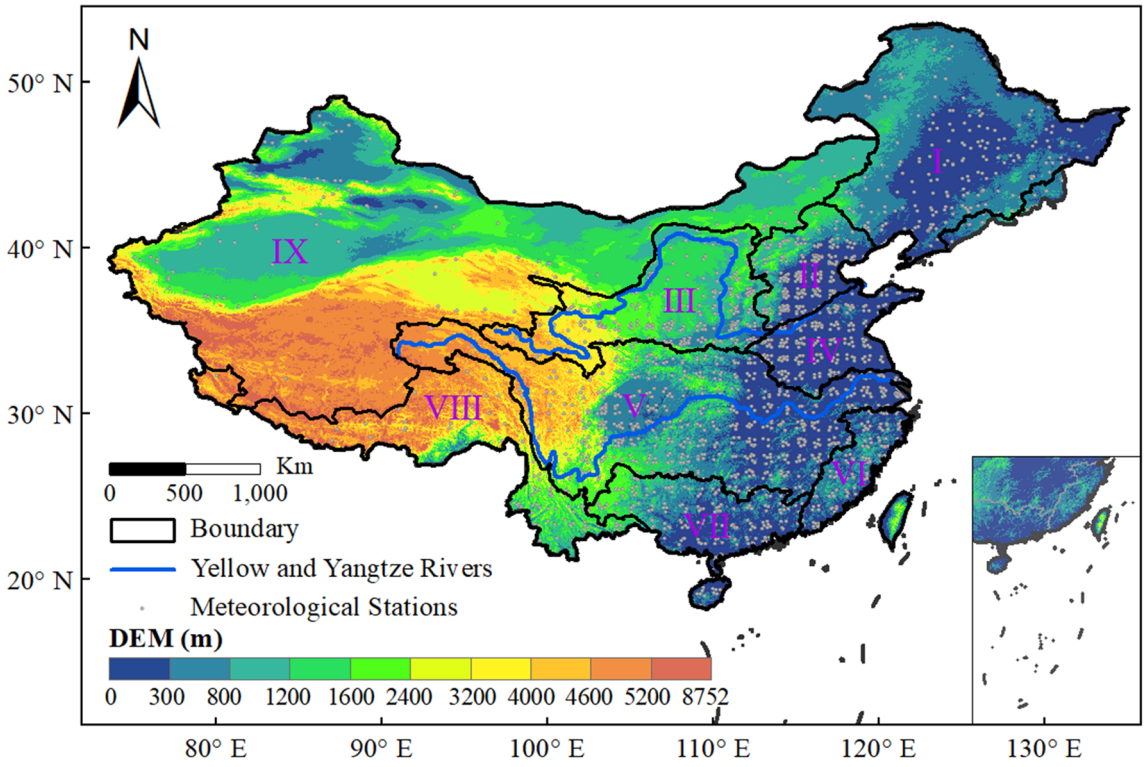

Fig. 1 Locations of the nine large river basins and meteorological stations. (I) Songhuajiang and Liaohe River basin; (II) Haihe River basin; (III) Yellow River basin; (IV) Huaihe River basin; (V) Yangtze River basin; (VI) Rivers in Southeast China basin; (VII) Pearl River basin; (VIII) Rivers in Southwest China basin; (IX) Rivers in Northwest China basin

Table 1 List of 8 CMIP6 GCMs used in this paper and their spatial resolution

Code	Model	Modeling center	Spatial resolution
1	CanESM5	Canadian Centre for Climate Modelling and Analysis, Canada	128 * 64
2	GFDL-ESM4	Geophysical Fluid Dynamics Laboratory, USA	288 * 180
3	IPSL-CM6A-LR	Institut Pierre-Simon Laplace, France	144 * 143
4	MIROC6	Atmosphere and Ocean Research Institute (The University of Tokyo), National Institute for Environmental Studies, and Japan Agency for Marine-Earth Science and Technology, Japan	256 * 128
5	MIROC-ES2L	Japan Agency for Marine-Earth Science and Technology, Atmosphere and Ocean Research Institute (The University of Tokyo), and National Institute for Environmental Studies, Japan	128 * 64
6	MRI-ESM2-0	Meteorological Research Institute, Japan	320 * 160
7	UKESM1-0-LL	UK Natural Environment Research Council centres and the Met Office Hadley Centre, UK	192 * 144
8	CAMS-CSM1-0	Chinese Academy of Meteorological Sciences	320 * 160

$$x_{correct} = x + \Delta \quad (2)$$

where x was precipitation; F referred to the cumulative distribution function (CDF) and F^{-1} referred to the inverse CDF; oc was observations during the training period; mc

was model outputs during the training period; *ms* was model outputs in a correction period.

All the bias-corrected series were downscaled statistically to a common grid of 0.5° × 0.5° longitude and latitude by the spatial disaggregation (SD) method. SD is applied based on the fundamental assumption that the statistical relationship will remain unchanged in the future (Su et al. 2018; Wang and Chen 2013b). Firstly, 0.5° gridded observed precipitation over China was interpolated to CMIP6 coarse resolution using a bilinear interpolation approach based on their multi-year averaged mean. Anomaly fields between the observed and bias-corrected model outputs were defined as the ratio of CMIP6 output to observation. Then, the coarse resolution anomaly fields of precipitation were interpolated to 0.5° resolution using a bilinear interpolation approach, and the interpolated anomaly fields were applied to 0.5°gridded observed precipitation to get the downscaled CMIP6 outputs. Accordingly, the CMIP6 models' data hereafter shown in this study are all bias-corrected. The bias correction and statistical downscaling could improve the accuracy of CMIP6 outputs in reproducing the observed spatial pattern and a long-term average of precipitation (Su et al. 2018). Even after bias correction, due to possible differences in the internal structure of the models or the applied initial conditions, the responses of the models are different to the same internal variability (which is dominant for precipitation) (Katiraie-Boroujerdy et al. 2019). To avoid this problem, the arithmetic ensemble mean method was used to calculate the MME mean of bias-corrected CMIP6 models.

The Taylor diagram was adopted to assess the simulation of all the bias-corrected CMIP6 climate patterns. The Taylor diagram could provide a concise statistical summary of how accurately patterns will match each other in terms of their standard deviation, centered root-mean-square (RMS) difference, and correlation (Taylor 2001).

The standard deviations σ of observed data and models were calculated as follows:

$$\sigma_{obs} = \sqrt{\frac{1}{N}\sum_{n=1}^{N}\left(X_{obsn} - \overline{X_{obs}}\right)^2} \tag{3}$$

$$\sigma_{model} = \sqrt{\frac{1}{N}\sum_{n=1}^{N}\left(X_{n} - \overline{X}\right)^2} \tag{4}$$

where $\overline{X_{obs}}$ and $\overline{X}$ denoted the mean values of observation and models, respectively.

The centered pattern RMS difference E was defined by (Cheng 2016):

$$E = \sqrt{\frac{1}{N}\sum_{n=1}^{N}\left[\left(X_n - \overline{X}\right) - \left(X_{obsn} - \overline{X_{obs}}\right)^2\right]} \tag{5}$$

The correlation coefficient r between observed data and models was defined as:

$$r = \left[\frac{1}{N}\sum_{n=1}^{N}\left(X_n - \overline{X}\right)\left(X_{obsn} - \overline{X_{obx}}\right)\right] / \left(\sigma_{model}\sigma_{obs}\right) \tag{6}$$

The key to constructing such a diagram was to recognize the relationship between the four statistical quantities of interest here (Taylor 2001):

$$E^2 = \sigma_{obs}^2 + \sigma_{model}^2 - 2\sigma_{obs}\sigma_{model}r \tag{7}$$

3 Results

3.1 Evaluation of CMIP6 simulated precipitation with observed data

Evaluation of annual mean precipitation simulations from the ensemble and individual CMIP6 models against the observed data indicated that the patterns of the simulated precipitation based on the bias-corrected CMIP6 models were similar to that of the observed precipitation over entire China (Fig. 2). Note that the annual mean precipitation in the southwestern edge of the Southwest River basin has been significantly overestimated for all the bias-corrected CMIP6 models, including the MME value (Fig. 2b–j). Meanwhile, the precipitation has been overvalued in Taiwan while undervalued in Hainan province. Overall, the MME and all the CMIP6 models showed good performance in China. On the national level, the annual precipitation decreased gradually from the southeast (> 1400.0 mm) to the northwest (< 400.0 mm) from 1961 to 2014 (Fig. 2). The historical precipitation in the Haihe River, Yellow River, Song-Liao River, and Northwest River basins was lower than 700 mm, while the precipitation over the Southeast River, Huaihe River, south Southwest River, middle and lower Yangtze River, and Pearl River basins was higher than 700.0 mm. Generally, the historical precipitation in south China was higher than that in north China.

The difference ratios in annual mean precipitation between eight CMIP6 models, their MME, and observations were presented in Fig. 3. Compared with the observations, east China exhibited better correspondence than west China from 1961 to 2014, where the mean bias between modeled and observed precipitation was less than ± 10%. The difference ratios were even less than ± 5% in

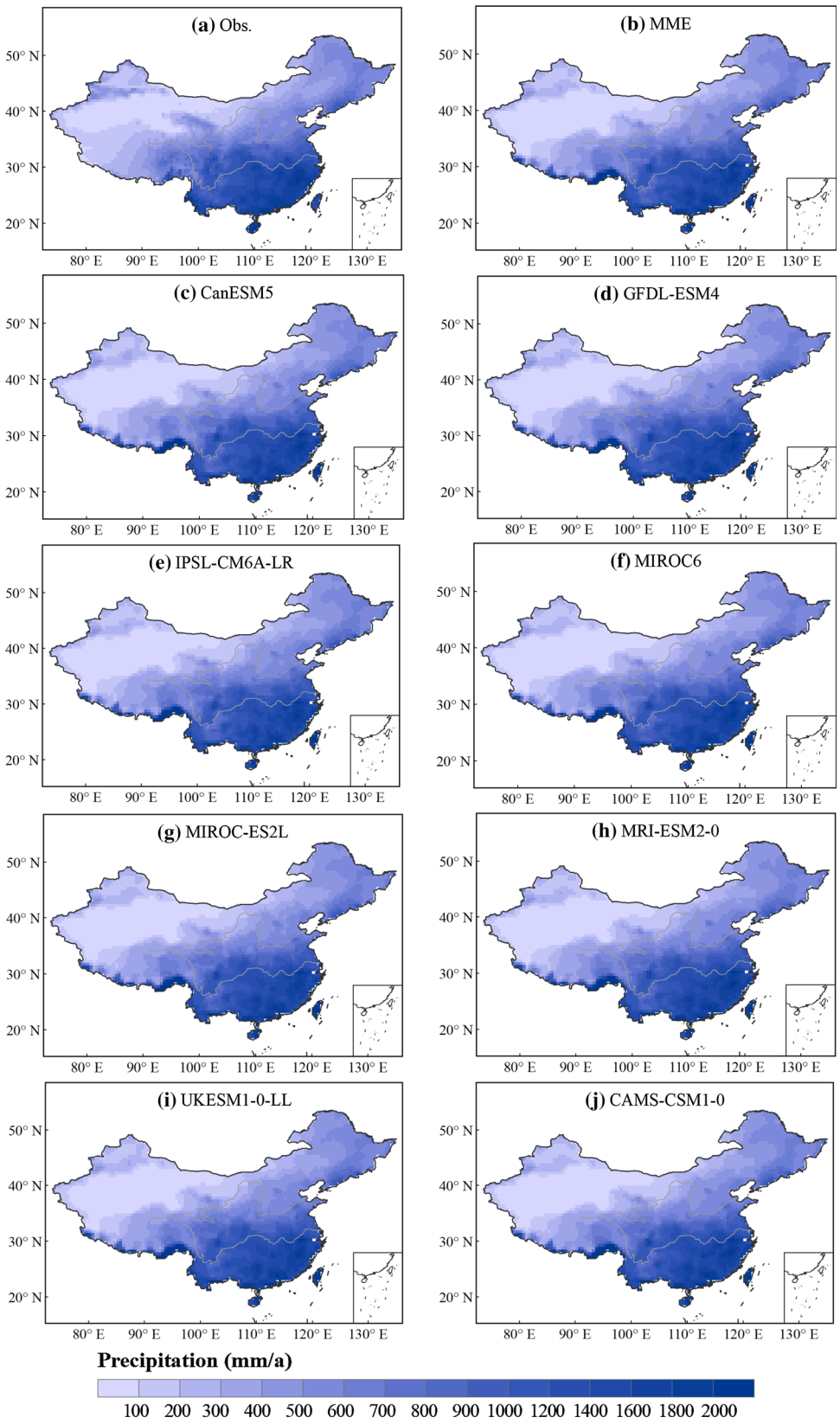

Fig. 2 Spatial distribution of annual mean precipitation over China during the period of 1961–2014 generated from **a** the observation (Obs.), and **b** the multi-model ensemble (MME) averaged from **c** CanESM5, **d** GFDL-ESM4, **e** IPSL-CM6A-LR, **f** MIROC6, **g** MIROC-ES2L, **h** MRI-ESM2-0, **i** UKESM1-0-LL, **j** CAMS-CSM1-0

many places of east China, which could be ignored. For west China, the bias in the high elevations of the Northwest River basin exceeded − 60%. Meanwhile, there was a larger positive bias in the southwestern edge regions of the

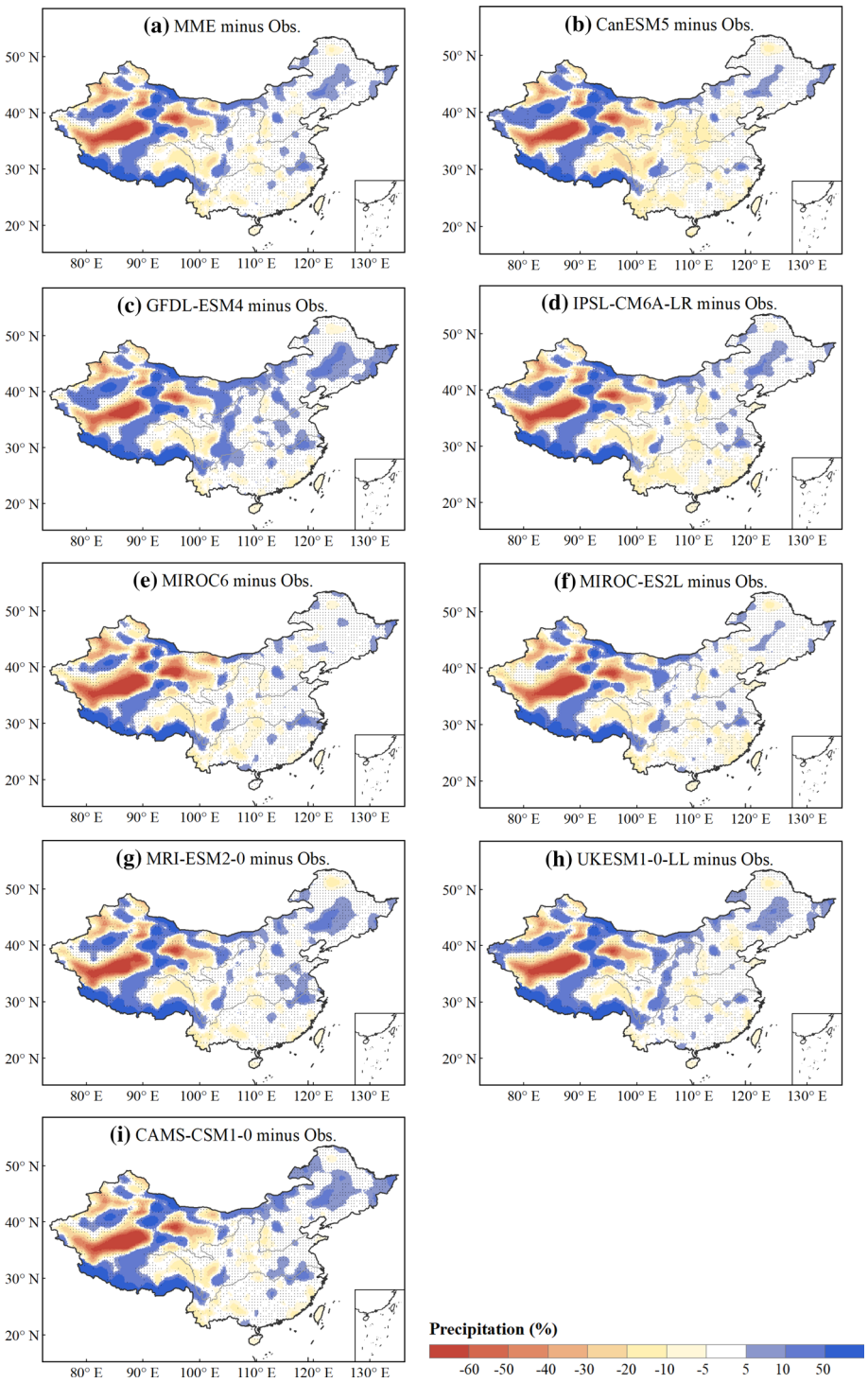

Fig. 3 The difference ratios in annual mean precipitation between 8 CMIP6 GCMs, MME, and observations during the period of 1961–2014. The dots indicate the difference was estimated at the 95% confidence level based on T-test

Southwest River basin (exceeded 50%), which occurred in Fig. 2 as well. Overall, as was shown in Table 2, MME and MIROC6 owned the lowed bias (difference ratio between − 5% and 5%: 35.10% and 35.77%, respectively). On the contrary, the bias was more prominent in IPSL-CM6A-LR (difference ratio less than − 50%: 5.34%; difference ratio more than 50%: 5.13%), MRI-ESM2-0 (difference ratio less than − 50%: 5.26%; difference ratio more than 50%: 4.91%), and CAMS-CSM1-0 (difference ratio less than − 50%: 5.26%; difference ratio more than 50%: 4.91%).

For temporal variability, the Taylor diagrams were presented in Fig. 4 to evaluate the accuracy of bias-

Table 2 Comparison of the percentage of grids for different difference ratios between modeled and observed annual mean precipitation over China (unit: %)

Model	≤ − 50	− 50 to − 10	− 10 to − 5	− 5 to 5	5–10	10 –50	≥ 50
MME	5.16	19.09	9.88	35.10	11.63	14.34	4.81
CanESM5	4.75	23.42	11.52	32.65	8.40	13.94	5.32
GFDL-ESM4	4.40	15.90	7.68	32.30	13.64	20.52	5.56
IPSL-CM6A-LR	5.34	21.19	10.96	32.71	10.74	13.94	5.13
MIROC6	6.18	21.37	10.58	35.77	10.47	11.65	3.97
MIROC-ES2L	5.42	21.35	11.49	34.61	10.18	12.67	4.27
MRI-ESM2-0	5.26	18.61	9.10	33.67	12.46	15.98	4.91
UKESM1-0-LL	4.86	18.39	9.61	33.86	11.47	16.76	5.05
CAMS-CSM1-0	5.26	19.31	8.14	32.01	13.48	16.89	4.91

corrected trends relative to observed precipitation trends over nine large river basins and the whole of China during 1961–2014. The correlations between eight bias-corrected CMIP6 models with observed data were more than 0.70 in most basins of China, except for the Huaihe River and the Southeast River basins. The correlation coefficients were more than 0.94 for the entire China (Fig. 4a). The centered RMS differences were low in the Northwest River basin (the differences were all lower than 6.80; Fig. 4j), while quite high in the Southeast River basin (the differences were all higher than 57; Fig. 4g). For individual CMIP6 models, the correlation coefficients for UKESM1-0-LL ($0.65 < r_{UKESM1-0-LL} < 0.95$) and MIROC6 ($0.61 < r_{MIROC6} < 0.95$) were comparatively high. The centered RMS differences of UKESM1-0-LL ($6.30 < E_{UKESM1-0-LL} < 77.65$) and MIROC6 ($6.02 < E_{MIROC6} < 81.15$) were relatively low. Generally, bias-corrected UKESM1-0-LL and MIROC6 showed the best performance among eight bias-corrected CMIP6 outputs in terms of describing the temporal variability. However, the two bias-corrected models did not perform well in all basins. In the Huaihe River, Southeast River, and Pearl River basins, UKESM1-0-LL performed the best. In the Haihe River, Yangtze River, and Northwest River basins, MIROC6 was superior to other bias-corrected models. In the Song-Liao River and Yellow River basins, GFDL-ESM4 performed the best. As for the entire China, IPSL-CM6A-LR showed the best performance. Whereas, the MME owned the highest similarity with observation, with 0.79 in the Southeast River basin and higher than 0.83 in other basins. Similarly, the MME presented the lowest centered RMS differences ($5.22 < E_{MME} < 57.07$) in all regions. Therefore, the MME showed the best performance in nine representative river basins and the whole of China from 1961 to 2014, especially in the entire China ($\sigma_{MME} = 35.83$, $E_{MME} = 8.00$, $r_{MME} = 0.98$) and the Northwest River basin ($\sigma_{MME} = 11.08$, E_{MME}=5.22,$r_{MME} = 0.96$) (Fig. 4a, j)

The progression of annual mean precipitation anomalies over nine large river basins and entire China during 1961–2099 has been shown in Fig. 5 indicating the inter-annual trend of precipitation fluctuations. As the MIROC6, UKESM1-0-LL, and MME showed better agreement with observed data analyzed above (Table 2; Fig. 4), only the inter-annual trend of observed precipitation, MIROC6 (Fig. 5a1–j1), UKESM1-0-LL (Fig. 5a2–j2), and MME (Fig. 5a3–j3) value were presented from 1961 to 2014. It could be seen that the precipitation showed significant increasing trends in the Northwest River basin during 1961–2014 based on MIROC6 and observed data (Fig. 5j1, j2, j3). However, this upward trend did not occur in UKESM1-0-LL and MME (Fig. 5j2,j3). Meanwhile, the precipitation from MME presented a slightly decreasing trend in the Yangtze River and Southeast River basins. Large interannual variations existed in precipitation, but the precipitation fluctuations in MME were much smaller. Overall, MIROC6 was superior in the Yangtze River basin (Fig. 5f1), while UKESM1-0-LL was superior in the Huaihe River basin (Fig. 5e2).

3.2 Projection of the precipitation in China's large river basin

As shown in Fig. 5, the precipitation fluctuations will increase during 2015–2099 over nine representative river basins and the whole of China, with some differences between low SSPs (SSP1-1.9 and SSP1-2.6) and high SSP (SSP5-8.5) scenarios. Generally, the higher SSP scenario meant higher precipitation by the end of the century, except for the southeastern regions of China. For example, the difference between the precipitation of MME in SSP5-8.5 and SSP1-1.9 was 231.1 mm in 2099 over the Southwest River basin, while the difference was 205.2 mm between SSP5-8.5 and SSP1-2.6 (Fig. 5i3). However, in 2099, SSP5-8.5 and SSP1-1.9 showed a -60.4 mm precipitation difference in the Southeast River basin (Fig. 5g3). Meanwhile, SSP5-8.5 and SSP1-2.6 presented − 98.8 mm,

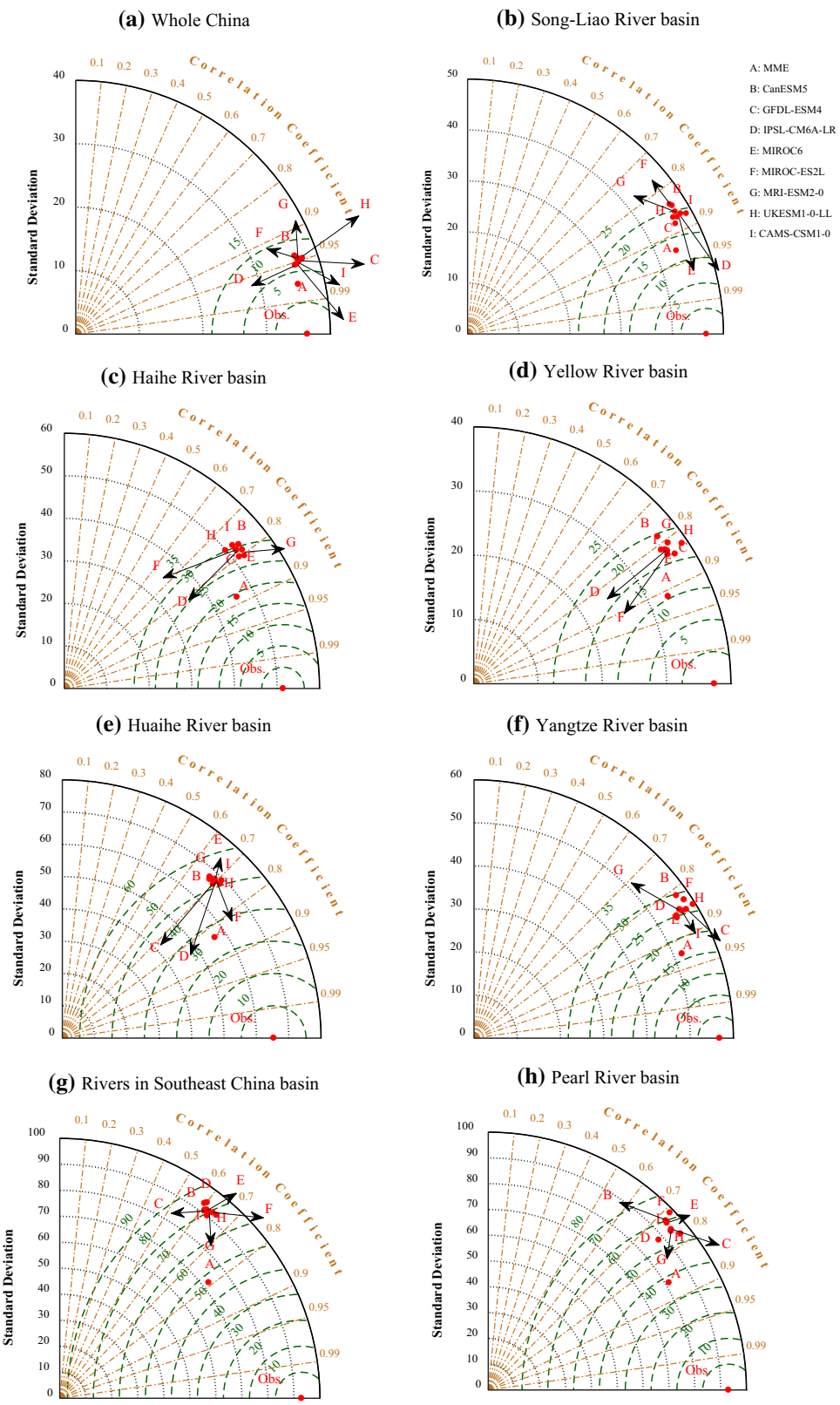

Fig. 4 Taylor diagrams for mean precipitation between observation, MME value, and eight bias-corrected CMIP6 models (indicated by the head of each arrow) during the period 1961–2014 over **a** whole China, and **b**–**j** the nine river basins. Dotted lines corresponded to standard deviations; dashed lines for centered RMS differences; dot-dash lines corresponded to correlations

− 39.0 mm, and − 85.0 mm precipitation differences of MME over the Huaihe River basin, Yangtze River basin, and Southeast River basin, respectively (Fig. 5e3–g3). Overall, the mean precipitation of China was expected to increase over the twnety first century under all the SSPs scenarios for the three modeled outputs. However, the

Fig. 4 continued

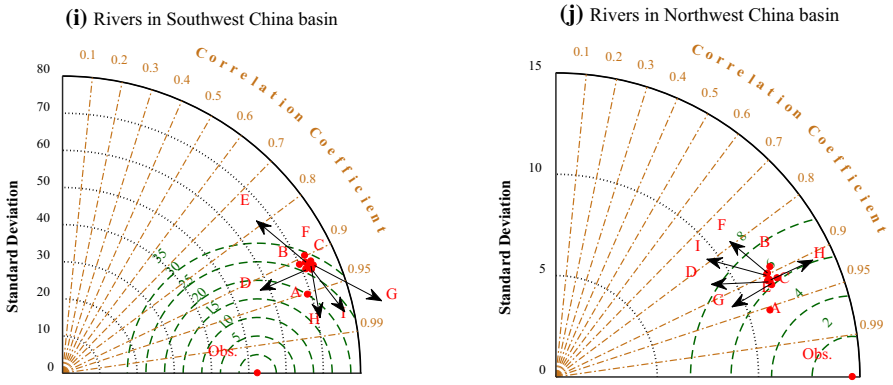

increase of precipitation over north China was higher than that in south China. The increase of precipitation over the Northwest River basin would even reach over 57.44% in the 2090s under SSP5-8.5 (Fig. 5j1–j3). Considering the bias in the Southwest River basin, the estimated increase in precipitation will be under 30% in south China by the end of the century under all SSPs scenarios (Fig. 5i1–i3).

We further explored the precipitation variations over nine large river basins and the whole of China during different future periods under five SSPs scenarios in detail (Fig. 6). The period of 1961–2010 was selected as the baseline period. During 2011–2020, the precipitation of MIROC6 and MME was lower than that in the baseline period over the Yangtze River basin (− 5.32 to − 0.26%) and Southeast River basin (− 6.53% to − 0.06%) under all SSPs scenarios. However, as for UKESM1-0-LL, the decrease of precipitation relative to the base period occurred in the Song-Liao River, Huaihe River, Southeast River, Pearl River, and Southwest River basins. Overall, relative to the base period, the three modeled precipitation all showed a downward trend during the 2010s in the Southeast River (Fig. 6g1–g3) and Pearl River (Fig. 6h1–h3) basins which were located in the southeast of China. In the Haihe River (Fig. 6c1–c3) and Northwest River (Fig. 6j1–j3) basins, the three modeled precipitation was always higher than that before 2010, including the 2010s. The higher emission scenario did not mean more precipitation. However, there will be more precipitation under the SSP5-8.5 scenario than the SSP1-1.9 and SSP1-2.6 scenarios after 2060, except for the Huaihe River, Yangtze River, Southeast River, and Pearl River basins. In general, more precipitation will occur in the future, especially in the Northwest River basin. The increasing trend of precipitation in north China will be larger than that in south China, as appeared in Fig. 5 as well. However, it will not reverse the distribution that the precipitation in south China (924.2–877.7 mm) is higher than that in north China (180.4–707.6 mm).

3.3 Uncertainty analysis of future precipitation projection

Box-and-whisker plots of future precipitation under different scenarios relative to the historical average (1961–2014) over nine representative river basins and the whole China, which were considered as an uncertainty visualization scheme were presented in Fig. 7 (Xiong 2017). It could be seen that the MME had the fewest outliers, especially in the Southwest River basin. For the Southwest River basin, the CMIP6 tended to overestimate the precipitation (Fig. 7i), consistent with our previous results (Figs. 2, 3). In contrast, the CMIP6 underestimated the annual mean precipitation in the Northwest River basin (Fig. 7j). Generally, the bias of the ensemble results was much lower than that of MIROC6 and UKESM1-0-LL, and the bias of low SSPs scenarios was relatively lower. However, in the Haihe River and Huaihe River basins, the bias of MIROC6 under medium SSPs scenarios was the lowest. In addition, Fig. 7 revealed that the difference between the SSP5-8.5 scenario and history was the largest except for the Yangtze River, Southeast River, and Pearl River basins.

Uncertainty ranges of precipitation from 1961 to 2099 relative to the historical average (1961–2014) over China and nine river basins were also demonstrated in Fig. 5a3–j3. The uncertainty ranges of projected precipitation fluctuations calculated by the arithmetic ensemble mean method were similar under the five SSPs scenarios. The ranges of eight bias-corrected model simulation estimations (the grey bars in the right of the figures) were almost the same as the uncertainty ranges of MME for all five scenarios. Therefore, the uncertainty range could not be narrowed using the arithmetic ensemble mean method in all basins under all scenarios. The magnitudes of the uncertainty ranges of precipitation fluctuations were inconsistent among different basins. The three southeastern basins (Yangtze River, Southeast River, and Pearl River

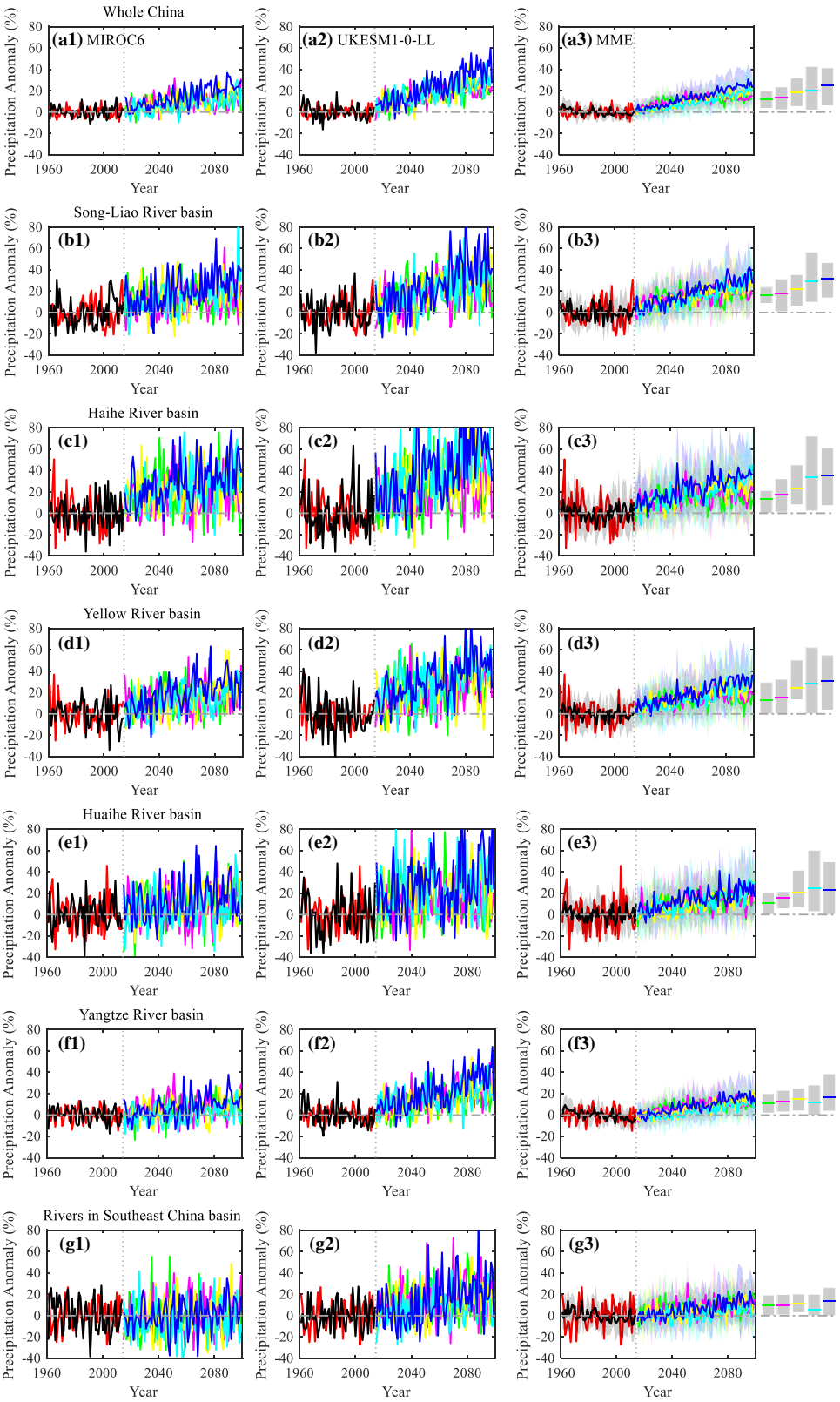

Fig. 5 Annual mean precipitation anomalies (%) from 1961 to 2099 over the **a1**, **a2**, **a3** whole China, and **b1**, **b2**, **b3**–**j1**, **j2**, **j3**) the nine river basins. The period 2015–2099 represented future projection scenarios from different SSPs. The shaded region represented the ± 1 standard deviation range of individual model annual averages. The grey bars in the right of the figures represented the range of 8 model simulation estimations for the mean precipitation during 2090–2099

basins) depicted the smallest uncertainty ranges (17.43–39.24%, Fig. 5f3–h3). In contrast, over the Northwest River basin, larger uncertainty ranges of precipitation change (29.69–79.26%) were detected (Fig. 5j3). This might be due to the low precipitation in north China, as the baseline of precipitation was small and the uncertainties of

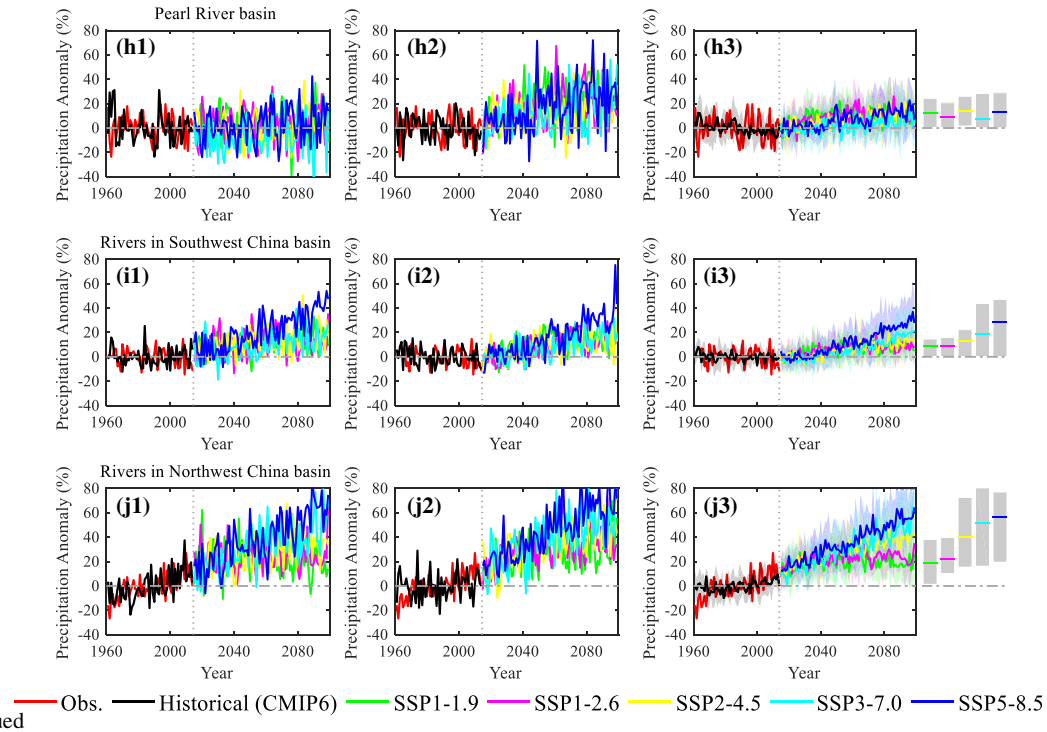

Fig. 5 continued

precipitation changes would be relatively large. This situation might also be attributed to a lack of meteorological stations in the Northwest River basin (Fig. 1).

4 Discussions

The outputs of global climate models are always biased and unable to predict future climate trends with great accuracy (Wu et al. 2017). Thus, bias correction and statistical downscaling were used to improve the accuracy of CMIP6 outputs in reproducing the observed spatial pattern and a long-term average of precipitation (Su et al. 2018). However, due to possible differences in the internal structure of the models or the applied initial conditions, the responses of the models are different to the same internal variability even after bias correction (Katiraie-Boroujerdy et al. 2019). To avoid this problem, according to the arithmetic ensemble mean approach, the MME of eight bias-corrected GCMs from CMIP6 was used in this study to project the precipitation variabilities under five SSPs scenarios over entire China and nine large basins. Interannual variations could be suppressed in the model mean (Knutti and Sedláček 2013). The results showed that, generally, all the eight bias-corrected CMIP6 outputs captured the spatial pattern of observed precipitation well, especially MIROC6. However, there was a low agreement between observed precipitation and the CMIP6 simulations in west china, which has been discovered in a previous study (Chen and Frauenfeld 2014). The annual mean precipitation in the southwestern edge of the Southwest River basin has been significantly overestimated for all bias-corrected models, including the MME ($> 50\%$), which occurred in CMIP5 models as well (Chen and Frauenfeld 2014; Su et al. 2013). Meanwhile, the bias in the high elevations of the Northwest River basin exceeded -60%. This underestimation presented disagreement with the results of Sun et al. (2015) and Ou et al. (2013), which might be due to the revision of CMIP6. The bias of west China was likely due to the coarse resolution of models, difficult to fully reproduce the processes like local circulation in complex topography (Su et al. 2013). This might be also due to the induced error during the interpolation process. The SD method is dependent on the observed data (Wang and Chen 2013b), so the lack of meteorological stations in western China could cause a huge bias there. Compared to the observation, the modeled precipitation has been slightly undervalued in most parts of south China ($< 10\%$), which was similar to the results by Sun et al. (2015). This situation was also in accordance with the underestimation of extreme precipitation in southern China (Ou et al. 2013). For temporal variability, MIROC6 and UKESM1-0-LL performed the best among eight bias-corrected CMIP6 models, showing higher correlation coefficients of 0.61–0.95 and 0.65–0.95, and lower centered RMS differences of 6.02–81.15 and 6.30-77.65. However, the two bias-corrected models did not perform the best in all basins. In the Haihe River, Yangtze River, and Northwest River basins,

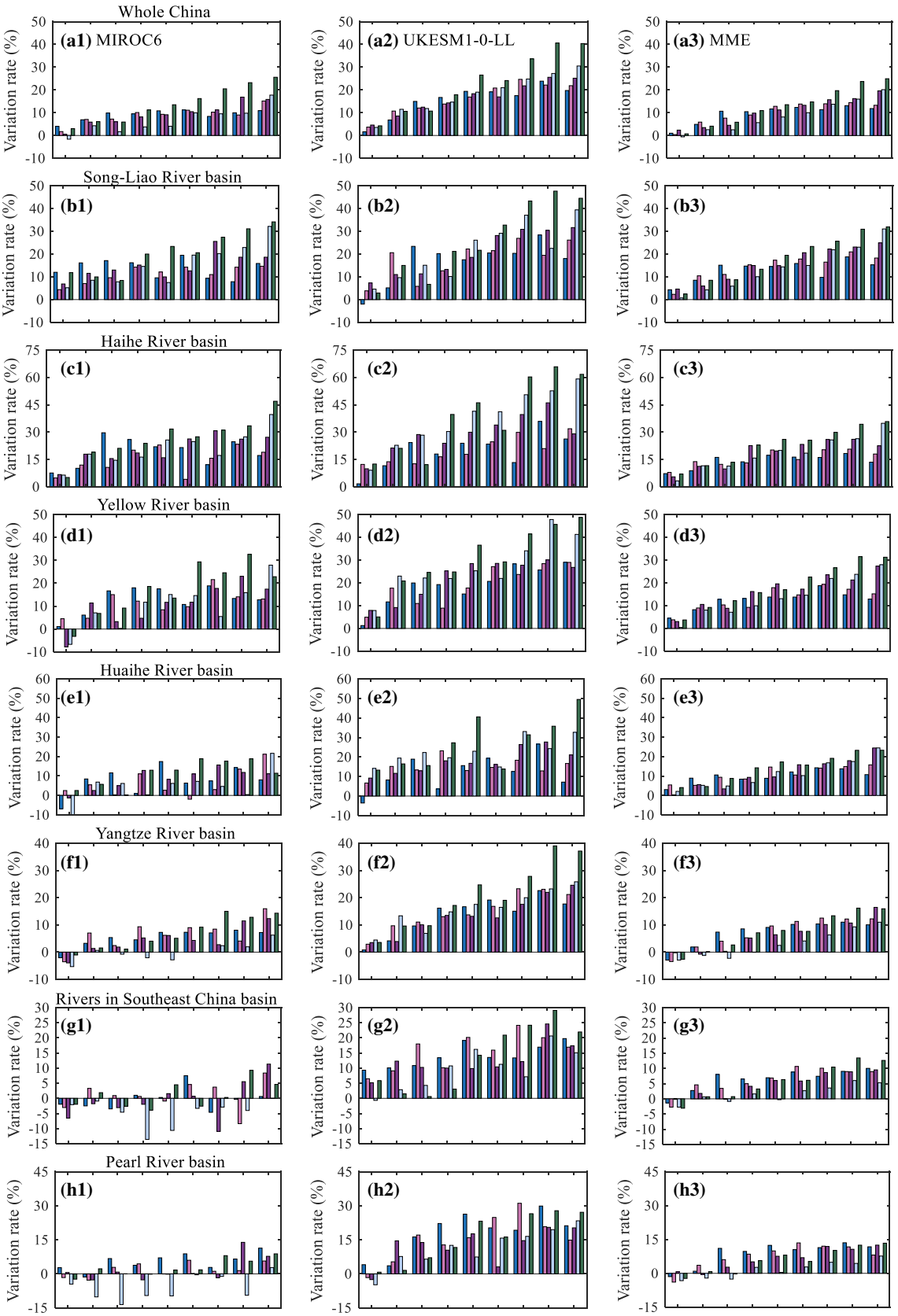

Fig. 6 Precipitation variation rate from MIROC6, UKESM1-0-LL, and MME during different future periods relative to 1961–2010 under five SSPs scenarios

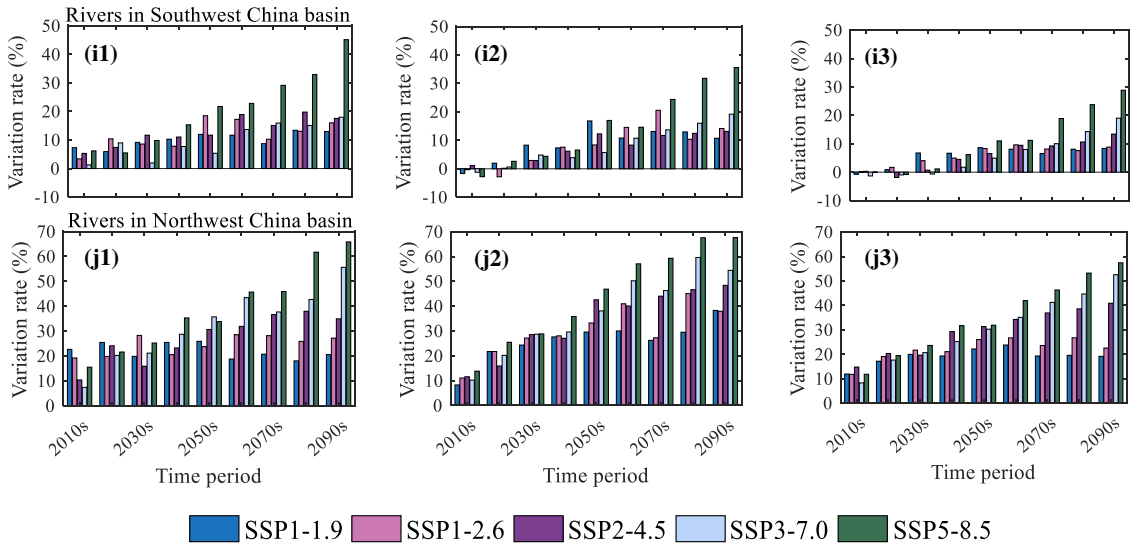

Fig. 6 continued

bias-corrected MIROC6 was superior to other bias-corrected models. In the Huaihe River, Southeast River, and Pearl River basins, bias-corrected UKESM1-0-LL performed the best. The MME of eight bias-corrected CMIP6 models presented a better agreement with observations than individual bias-corrected CMIP6 models. There were small centered RMS differences in precipitation in MME ($5.22 < E_{MME} < 57.07$) compared to individual CMIP6 models. Meanwhile, the MME of eight bias-corrected models showed close correlation ($0.79 < 0.79 < r_{MME} < 0.98$) with the observed data over nine representative river basins and the whole of China. These findings are consistent with previous studies emphasizing that the MME techniques can reduce the uncertainty of independent models effectively with better performance (Feng et al. 2011; He et al. 2018; Katiraie-Boroujerdy et al. 2019; Sun et al. 2015) described that the trend of observations appeared in MME projections was much better than any individual model, but it contained a significant deviation. Overall, the precipitation fluctuations and bias of MIROC6 and UKESM1-0-LL were greater than those of MME.

Spatially, higher precipitation in south China (> 700.0 mm) compared to north China (< 700.0 mm) was observed during 1961–2014. Temporally, huge inter-annual variations existed in the evolution of precipitation variabilities over nine large river basins and the whole of China. Under all SSPs scenarios, the precipitation would increase over entire China during 2015–2099. The increase over north China will be higher than that in south China under all SSPs scenarios. Some country-scale studies on precipitation projection based on CMIP5 revealed the same results that the precipitation will increase significantly over most regions of China, and the increase in northern China will be greater than that in southern China (Chen and Frauenfeld 2014; Wang and Chen 2013a; Xu and Xu 2012). Similarly, Wang et al. (2018) pointed out that annual precipitation will increase in the 2080s under RCP8.5 and RCP4.5 scenarios over northeastern China. For MIROC6, UKESM1-0-LL and the MME, the increase in precipitation will even reach over 57.44% in the Northwest River basin in the 2090s under the SSP5-8.5 scenario. This upward tendency of precipitation in northwest China might further alleviate the pressure of water shortage there, but the upward trend in southeast China might aggravate the risk of flood-induced disasters in these regions (Zheng et al. 2019). In the Yangtze River and Southeast River basins, the precipitation of MIROC6 and MME in the 2010s was all lower than that during 1961–2010 (− 6.53 to − 0.06%) irrespective of high SPPs or low SSPs scenarios. According to this phenomenon, Sun et al. (2015) indicated that the precipitation will decrease in the two basins during 2011–2030 for all RCPs and increase substantially thereafter, because the enhanced monsoon circulation had a two-stage evolution during 2010–2099 with a prominent increase after the 2040s. However, the precipitation of UKESM1-0-LL was lower than that in the baseline period over the Song-Liao River, Huaihe River, Southeast River, Pearl River, and Southwest River basins during the 2010s. Overall, the three modeled precipitation all showed a downward trend during the 2010s in the Southeast River and Pearl River basins. In addition, there would be more precipitation under the SSP5-8.5 scenario than SSP1-1.9 and SSP1-2.6 scenarios after 2060, except for the Huaihe River, Yangtze River, Southeast River, and Pearl River basins.

Uncertainties in climate models have often been a limiting factor, in particular on local scales (Knutti and

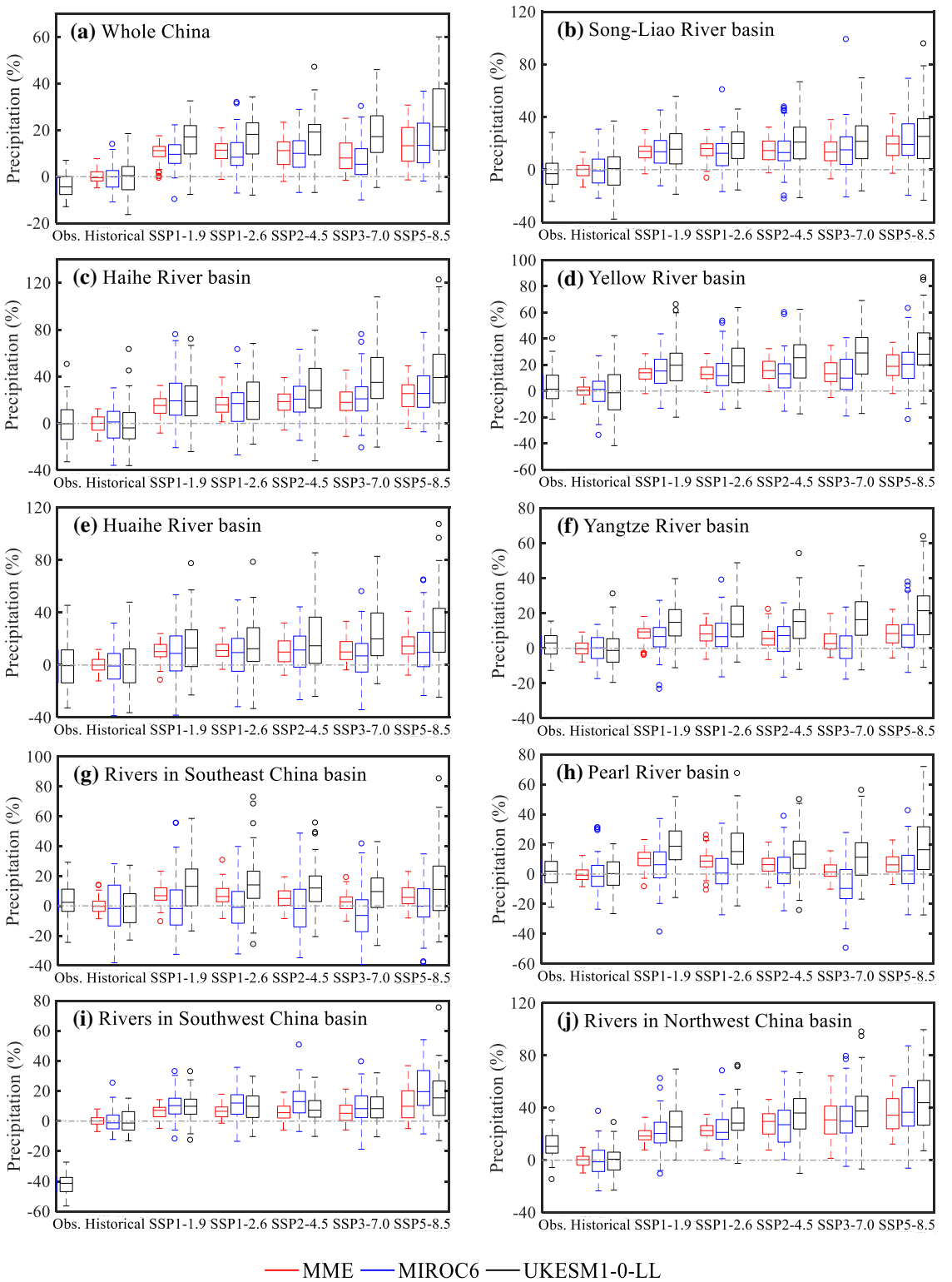

Fig. 7 Box-and-whisker plots for future precipitation under different scenarios along with observed and historical simulated precipitation data sets relative to the historical average (1961–2014) over the **a** whole China, and **b–j** the nine river basins. The circles were outliers

Sedláček 2013). However, the uncertainties of global climate models are unavoidable (Hawkins and Sutton 2010). In this paper, the uncertainty ranges for precipitation estimation could not be effectively narrowed by using the arithmetic ensemble mean method. The uncertainty ranges of precipitation fluctuations in north China are larger

(15.31–79.26%), while they are smaller in south China (16.06–57.55%). This might be due to the low baseline of precipitation in north China. In addition, both aerosols forcing in the emission scenarios and aerosol-cloud module of GCMs could impact the precipitation simulation and projections (Lin et al. 2016, 2018). These results are similar to the projections of CMIP5 precipitation over China using the reliability ensemble average approach (Sun et al. 2015; Lehner et al. 2019) revealed that precipitation changes were more uncertain as well. Generally, the bias of the ensemble results was much lower than that of MIROC6 and UKESM1-0-LL, and the bias of low SSPs scenarios was relatively lower. However, in the Haihe River and Huaihe River basins, the bias of MIROC6 had the lowest bias under medium SSPs scenarios. The uncertainties could result in low confidence in regional projections of precipitation (Smith et al. 2020). Therefore, more attention should be paid to more reliable GCMs and better methods of narrowing uncertainties.

5 Conclusions

In this study, we analyzed the changes of precipitation during 1961–2099 over nine large river basins of China based on eight CMIP6 models bias-corrected by the method of EDCDF under SSP1-1.9, SSP1-2.6, SSP2-4.5, SSP3-7.0, and SSP5-8.5 scenarios. The major conclusions were summarized as follows:

1. Generally, all the bias-corrected CMIP6 models captured the spatial pattern of the precipitation well in China during 1961–2014. However, the simulated annual mean precipitation of CMIP6 outcomes has been significantly overvalued in the Southwest River basin (> 50%), while it was undervalued in the high elevations of the Northwest River basin (< -60%). Among all the models, the MIROC6 and UKESM1-0-LL models have a better performance in simulating precipitation over China with higher correlation coefficients of 0.61–0.95 and 0.65–0.95, respectively. The MME of eight bias-corrected CMIP6 models showed better agreement with observed precipitation than individual CMIP6 model in all nine river basins during the period 1961–2014 with the lowest centered RMS differences ($5.22 < E_{MME} < 57.07$) and the highest correlations ($0.79 < r_{MME} < 0.98$).
2. The precipitation will increase over the whole of China under all SSPs scenarios during 2015–2099. Moreover, the rate of precipitation increase over north China was higher than that in south China under all the SSPs scenarios. And the increase of precipitation in the Northwest River basin will reach over 57.44% in the 2090s under SSP5-8.5 for the MME. This upward tendency in north China might alleviate the shortage of water there, but will not change the pattern of more rain in the south (924.2–877.7 mm) and less in the north (180.4–707.6 mm).
3. In the southeastern river basins, the precipitation of MIROC6 and MME in the 2010s was all lower than that during 1961–2010 (− 6.53 to − 0.06%) under all SSPs scenarios. While the precipitation will increase obviously under all the SSPs scenarios, especially for the SSP5-8.5 scenario after the year of 2060.
4. Uncertainties were unavoidable for precipitation estimation. However, the bias of the MME was much lower than that of individual CMIP6 model, and the bias of lower SSPs scenarios was relatively lower. Generally, the uncertainty ranges of precipitation variability in north China (15.31–79.26%) were larger compared to south China (16.06–57.55%). There is still room for reducing the uncertainty of regional precipitation change prediction. Nevertheless, this paper revealed the projections of precipitation and disclosed the uncertainties of CMIP6 models over China, which will contribute to a better understanding of the evolution of regional precipitation in China and the world in the future.

Authors' contributions JT: Writing—Original draft preparation, Software, Data Curation; ZZ: Conceptualization, Writing—Review and Editing; ZA and LZ: Writing—Review and Editing; BS and TJ: Resources, Data curation; HT: Methodology. All authors read and approved the final manuscript.

Funding This work was supported by National Key Research and Development Project of China (2019YFC0409004); National Natural Science Foundation of China (41971025 and 41971023); West Light Foundation of the Chinese Academy of Sciences (2019-XBQNXZ-B-004 and 2019-XBYJRC-001) and the Priority Academic Program Development of Jiangsu Higher Education Institutions (PAPD).

Availability of data and material Not applicable.

Code availability Not applicable.

Compliance withe thical standards

Conflict of interest The authors declare no conflict of interest.

References

Chen L, Frauenfeld OW (2014) A comprehensive evaluation of precipitation simulations over China based on CMIP5 multimodel ensemble projections. J Geophys Res Atmos 119:5767–5786

Cheng YP (2016) The simulation assessment and prediction method research on the major modes of the Asian–Australian monsoon

interannual variability. Nanjing University of Information Science and Technology, Nanjing
Editorial (2019) The CMIP6 landscape. Nat Clim Change 9:727
Eyring V, Cox PM, Flato GM, Gleckler PJ, Abramowitz G, Caldwell P, Collins WD, Gier BK, Hall AD, Hoffman FM, Hurtt GC, Jahn A, Jones CD, Klein SA, Krasting JP, Kwiatkowski L, Lorenz R, Maloney E, Meehl GA, Pendergrass AG, Pincus R, Ruane AC, Russell JL, Sanderson BM, Santer BD, Sherwood SC, Simpson IR, Stouffer RJ, Williamson MS (2019) Taking climate model evaluation to the next level. Nat Clim Change 9:102–110
Feng JM, Lee D, Fu CB, Tang JP, Sato Y, Kato H, Mcgregor JL, Mabuchi K (2011) Comparison of four ensemble methods combining regional climate simulations over Asia. Meteorol Atmos Phys 111:41–53
Gemmer M, Becker S, Jiang T (2004) Observed monthly precipitation trends in China 1951–2002. Theor Appl Climatol 77:39–45
Hagedorn R, Doblas-Reyes FJ, Palmer TN (2005) The rationale behind the success of multi-model ensembles in seasonal forecasting—I. Basic concept. Tellus 57A:219–233
Han H, Zhang J, Ma G, Zhang X, Bai Y (2018) Advances on impact of climate change on ecosystem services. J Nanjing For Univ (Nat Sci Ed) 42:184–190
Hawkins E, Sutton R (2010) The potential to narrow uncertainty in projections of regional precipitation change. Clim Dyn 37:407–418
He L, Cleverly J, Wang B, Jin N, Mi CR, Liu DL, Yu Q (2018) Multi-model ensemble projections of future extreme heat stress on rice across southern China. Theor Appl Climatol 133:1107–1118
Heinze C, Eyring V, Friedlingstein P, Jones C, Balkanski Y, Collins W, Fichefet T, Gao S, Hall A, Ivanova D, Knorr W, Knutti R, Löw A, Ponater M, Schultz MG, Schulz M, Siebesma P, Teixeira J, Tselioudis G, Vancoppenolle M (2019) ESD reviews: climate feedbacks in the earth system and prospects for their evaluation. Earth Syst Dyn 10:379–452
Katiraie-Boroujerdy P, Akbari Asanjan A, Chavoshian A, Hsu K, Sorooshian S (2019) Assessment of seven CMIP5 model precipitation extremes over Iran based on a satellite-based climate data set. Int J Climatol 39:3505–3522
Knutti R, Sedláček J (2013) Robustness and uncertainties in the new CMIP5 climate model projections. Nat Clim Change 3:369–373
Lehner F, Wood AW, Vano JA, Lawrence DM, Clark MP, Mankin JS (2019) The potential to reduce uncertainty in regional runoff projections from climate models. Nat Clim Change 9:926–933
Lim Y, Lee J, Oh H, Kang H (2014) Independent component regression for seasonal climate prediction: an efficient way to improve multimodel ensembles. Theor Appl Climatol 119:433–441
Lin L, Wang Z, Xu Y, Fu Q (2016) Sensitivity of precipitation extremes to radiative forcing of greenhouse gases and aerosols. Geophys Res Lett 43:9860–9868
Lin L, Xu Y, Wang Z, Diao C, Dong W, Xie S (2018) Changes in extreme rainfall over india and china attributed to regional aerosol-cloud interaction during the late 20th century rapid industrialization. Geophys Res Lett 45:7857–7865
O'Neill BC, Kriegler E, Riahi K, Ebi KL, Hallegatte S, Carter TR, Mathur R, van Vuuren DP (2013) A new scenario framework for climate change research: the concept of shared socioeconomic pathways. Clim Change 122:387–400
O'Neill BC, Tebaldi C, van Vuuren DP, Eyring V, Friedlingstein P, Hurtt G, Knutti R, Kriegler E, Lamarque J, Lowe J, Meehl GA, Moss R, Riahi K, Sanderson BM (2016) The scenario model intercomparison project (ScenarioMIP) for CMIP6. Geosci Model Dev 9:3461–3482
Ou TH, Chen DL, Linderholm HW, Jeong JH (2013) Evaluation of global climate models in simulating extreme precipitation in China. Tellus A 65:19799
Smith DM, Scaife AA, Eade R, Athanasiadis P, Bellucci A, Bethke I, Bilbao R, Borchert LF, Caron LP, Counillon F, Danabasoglu G, Delworth T, Doblas-Reyes FJ, Dunstone NJ, Estella-Perez V, Flavoni S, Hermanson L, Keenlyside N, Kharin V, Kimoto M, Merryfield WJ, Mignot J, Mochizuki T, Modali K, Monerie PA, Müller WA, Nicolí D, Ortega P, Pankatz K, Pohlmann H, Robson J, Ruggieri P, Sospedra-Alfonso R, Swingedouw D, Wang Y, Wild S, Yeager S, Yang X, Zhang L (2020) North Atlantic climate far more predictable than models imply. Nature 583:796–800
Steinschneider S, Lall U (2015) A hierarchical Bayesian regional model for nonstationary precipitation extremes in Northern California conditioned on tropical moisture exports. Water Resour Res 51:1472–1492
Su FG, Duan XL, Chen DL, Hao ZC, Cuo L (2013) Evaluation of the global climate models in the CMIP5 over the Tibetan Plateau. J Clim 26:3187–3208
Su B, Huang J, Fischer T, Wang Y, Kundzewicz ZW, Zhai J, Sun H, Wang A, Zeng X, Wang G, Tao H, Gemmer M, Li X, Jiang T (2018) Drought losses in China might double between the 1.5 °C and 2.0 °C warming. Proc Natl Acad Sci 115:10600–10605
Sun QH, Miao CY, Duan QY (2015) Projected changes in temperature and precipitation in ten river basins over China in 21st century. Int J Climatol 35:1125–1141
Taylor KE (2001) Summarizing multiple aspects of model performance in a single diagram. J Geophys Res 106:7183–7192
van Vuuren DP, Edmonds J, Kainuma M, Riahi K, Thomson A, Hibbard K, Hurtt GC, Kram T, Krey V, Lamarque J, Masui T, Meinshausen M, Nakicenovic N, Smith SJ, Rose SK (2011) The representative concentration pathways: an overview. Clim Change 109:5–31
Wang L, Chen W (2013a) A CMIP5 multimodel projection of future temperature, precipitation, and climatological drought in China. Int J Climatol 34:2059–2078
Wang L, Chen W (2013b) Application of bias correction and spatial disaggregation in removing model biases and downscaling over China. Adv Earth Sci 28:1144–1153
Wang WG, Shao QX, Yang T, Yu ZB, Xing WQ, Zhao CP (2014) Multimodel ensemble projections of future climate extreme changes in the Haihe River Basin, China. Theor Appl Climatol 118:405–417
Wang Y, Bian JM, Zhao YS, Tang J, Jia Z (2018) Assessment of future climate change impacts on nonpoint source pollution in snowmelt period for a cold area using SWAT. Sci Rep 8:2402
Wu D, Yan DH (2013) Projections of future climate change over Huaihe River basin by multimodel ensembles under SRES scenarios. J Lake Sci 25:565–575
Wu YN, Zhong P, Xu B, Zhu FL, Fu JS (2017) Evaluation of global climate model on performances of precipitation simulation and prediction in the Huaihe River basin. Theor Appl Climatol 133:191–204
Xiong CY (2017) A research on correlation analysis of dimensional uncertainty. Tianjin Institute of Software Engineering, Tianjin
Xu C, Xu Y (2012) The projection of temperature and precipitation over China under RCP scenarios using a CMIP5 multi-model ensemble. Atmos Ocean Sci Lett 5:527–533
Zhang ZX, Chen X, Xu C, Yuan LF, Yong B, Yan SF (2011) Evaluating the non-stationary relationship between precipitation and streamflow in nine major basins of China during the past 50 years. J Hydrol 409:81–93
Zhang L, Karthikeyan R, Bai ZK, Wang JM (2017) Spatial and temporal variability of temperature, precipitation, and streamflow in upper Sang-kan basin, China. Hydrol Process 31:279–295

Zhang LX, Chen XL, XIn XG, (2019) Short commentary on CMIP6 scenario model intercomparison project (ScenarioMIP). Clim Change Res 15:519–525

Zheng J, Fan JL, Zhang FC (2019) Spatiotemporal trends of temperature and precipitation extremes across contrasting climatic zones of China during 1956–2015. Theor Appl Climatol 138:1877–1897

Zhou L, Jiang ZH (2017) Future changes in precipitation over Hunan Province based on CMIP5 simulations using the statistical downscaling method of transform cumulative distribution function. Acta Meteorol Sin 75:223–235